ASEAN Engineering Journal

Full Paper

MECHANICAL TREATMENT ON ASTM A128 GRADE C WITH DISPERSED HARDENED AUSTENITE ON THE GRAIN

Mohammad Reza Hermawan[a, b]*, Budi Hartono Setiamarga[b]

[a]Mechanical Engineering Departemen, Faculty of Engineering, Pasundan University, Bandung, Indonesia
[b]Material Science and Engineering, Faculty of Mechanical and Aerospace Engineering, Bandung Institute of Technology, Bandung, Indonesia

Article history
Received
01 January 2024
Received in revised form
30 April 2024
Accepted
19 May 2024
Published online
30 November 2024

*Corresponding author
rezahermawan@unpas.ac.id

Graphical abstract

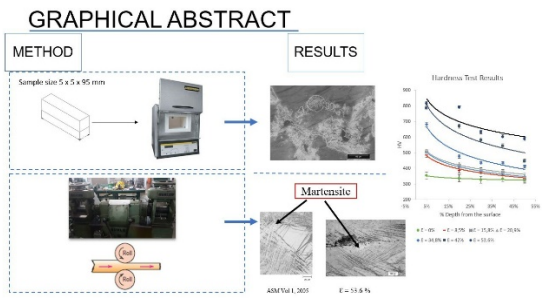

Abstract

This study examined the mechanical characteristics of ASTM A128 Grade C austenitic manganese steel with dispersed hardened austenite by cold rolling. Dispersed hardened austenite results from two-stage heating. The first stage heated, carbide at the grain boundaries transformed to pearlite at 625°C for 3.5 hours, while the second stage was heated at 1000°C for 1.5 hours and cooled with water to generate dispersed hardened austenite. Mechanical cold rolling on two-stage heated material develops martensite, as shown by XRD and qualitative magnetic tests. Hardness increased by 37% compared to two heating sessions. Even though cracks had developed over the cross-section, rolling to 53.6% increased hardness 132% more than two heating phases. Orange peeling, which occurs when the material's surface shrinks due to martensitic transformation, slip, and twinning, indicates that the surface is more brittle than the inside.

Keywords: austenitic manganese steel, cold rolling, dispersed hardened ausenite

1.0 INTRODUCTION

Sir Robert Hadfield introduced austenitic manganese steel in 1982, with a composition of 1.2% carbon and 12% manganese [1]. In the cast condition, austenitic manganese steel is very brittle due to the presence of carbide deposits, so it does not have sufficient physical properties to withstand impact. To improve the mechanical properties of austenitic manganese steel, researchers have explored various methods, such as adding alloying elements [2], applying heat treatment [3], and utilizing work hardening [4], [5], [6], [7], [8].

To obtain a full austenite structure, the cast structure of austenitic manganese steel requires solution treatment at the austenization temperature with a specific holding time and subsequent water quenching. The austenite phase grows due to the high content of manganese, which is an austenite stabilizer [3]. Austenization temperature and holding time are factors that greatly influence the desired final phase. When austenitic manganese steel that has received solution treatment experiences plastic deformation, there will be an increase in strength caused by the FCC lattice, which has more slip systems, which causes very large dislocation movements. This process is shown by a rise in the hardness value on the surface of austenitic manganese steel after it has been deformed plastically, either by impact load or abrasion [9]. The work hardening mechanism in austenitic manganese steel during tensile testing occurs due to plastic deformation caused by the twin mechanism and grain size [2]. When a twin mechanism occurs in an austenite grain, the grain will be divided into n-parts because of the twin planes that double each other, which can inhibit the movement of dislocations. The solution treatment process influences this strengthening mechanism through its dependence on grain size.

Ilham Lukman Nur Hakim and Budi Hartono Setiamarga (2020) conducted research on the formation of dispersed hardened austenite using a two-stage formation process [10]. The research found that toughness increases with increasing holding time in the first stage of heating, but it is accompanied by a decrease in yield strength. In this research, the focus is more on observing the effect of plastic deformation using the cold rolling method on ASTM A128 grade C austenitic manganese steel, which has been heated in two stages to form dispersed hardened austenite, both in terms of the strengthening mechanism formed and the increase in hardness that occurs.

2.0 METHODOLOGY

2.1 Material

ASTM A128 Grade C austenitic manganese steel was used in this research. In the as-cast condition, the high chrome content in this material causes more carbides to form at the grain boundaries. However, a large amount of carbide can help the formation of dispersed hardened austenite in the two-stage heating process because chromium is a carbide [2].

2.1 Method

The as-cast material is cut until the cross-section measures 5 x 5mm with a length of 100mm. Two stages of heating are performed on the cut material in the Nabertherm Muffle Furnace L3/11 with Flap Door heat treatment furnace, followed by rapid cooling with agitated water. The heating scheme used in the research is shown in Figure 1, where the first stage of heating is carried out at a temperature of 625°C for 3.5 hours and the second stage of heating is carried out at a temperature of 1000°C for 1.5 hours. Determination of the first stage of heating for 3.5 hours because its toughness is 17 times higher than the as-cast condition and lamellae have formed in the carbide area, which is a characteristic of pearlite [10].

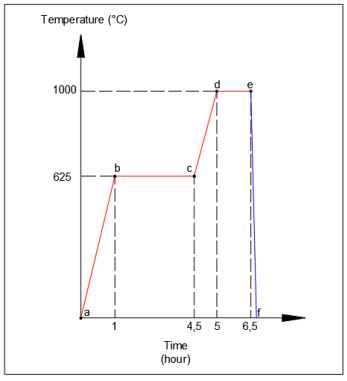

Figure 1 Two-stage heating process scheme

The samples, which have undergone a two-stage heating process, are subsequently subjected to cold rolling using a BUHLER Roll Mill. This rolling process is carried out in stages, with each stage resulting in a thickness decrease of 0.1mm. The rolling continues until fractures appear across the cross-section of the samples. The material characteristics were observed at strain reductions of 0%, 8.5%, 15.8%, 20.9%, 34.8%, 42%, and 53.6%. These values were determined using the equation $\varepsilon = ln\frac{L}{L_0}$ [11].

The microVickers FR-1e was utilized to conduct a hardness study of the specimen using a minor force of 98.07N, a major load of 980.7N, and a holding time of 15 seconds. We performed microstructural investigation using the metallographic technique described in ASTM E3-01, utilizing an optical microscope and scanning electron microscope (SEM) for enhanced magnification. X-ray diffraction (XRD) analysis was conducted to ascertain the structure developed in the material that underwent cold rolling. This was achieved by comparing the structure of the material that received only two stages of heating. We do magnetic testing using magnets on as-cast samples, materials subjected to only two steps of heating, and materials subjected to cold rolling.

3.0 RESULTS AND DISCUSSION

3.1 Microstructure Observation of As-cast Materials

The axle microstructure in austenitic manganese steel consists of carbide and austenite as the dominant matrix or phase [12]. The austenite phase that dominates the microstructure of austenitic manganese steel is caused by the high level of manganese, which is an austenite stabilizer [3]. The microstructure in this study provides information that the austenitic manganese steel material studied has an austenite phase with carbide in the form of a network in the form of lamellae [13], as shown in the Figure 2. The presence of carbides at grain boundaries is a problem in austenitic manganese steel materials because carbides have the properties of being brittle, making this austenitic manganese steel material not resistant to impact loads or abrasion. Referring to the Figure 2, many carbides are formed at grain boundaries, and the austenite phase is the main phase. This austenitic manganese steel has hyper-eutectoid properties, so cementite forms at the grain boundaries. Based on the Fe-Mn phase diagram, the γ (austenite) phase is formed from a liquid state, and as the solidification process progresses, the austenite phase transforms into γ (austenite) + Fe3C (cementite). Because this manganese steel is classified as hyper-eutectoid, this austenitic manganese steel has a tendency to form pre-eutectoid cementite, which is formed from γ (austenite) [13].

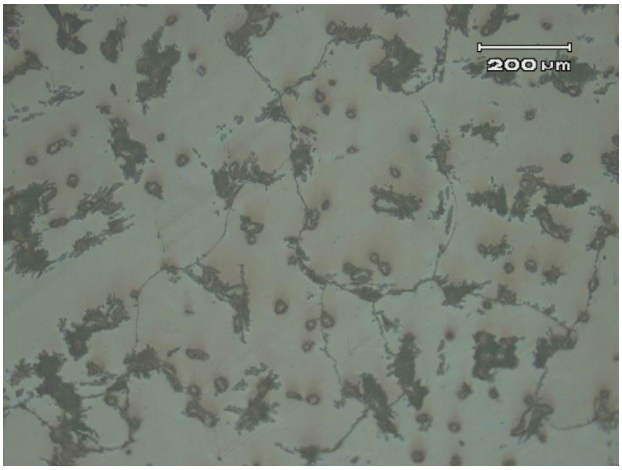

Figure 2 Microstructure of as-cast austenitic manganese steel

3.2 Microstructure Observation of Heat Treatment Results

A two-stage heat treatment has been carried out on the material with the aim of forming dispersed hardened austenite, which has high toughness characteristics. In the first stage of heating, carbide at the grain boundaries transforms into pearlite, which is formed from changes in the austenite phase at its eutectoid composition and temperature [14]. The process of forming pearlite in the first stage of heating is closely related to the dispersed hardened austenite that will be formed in the second stage because the morphology of pearlite greatly influences the size, shape, and distance between carbide colonies.

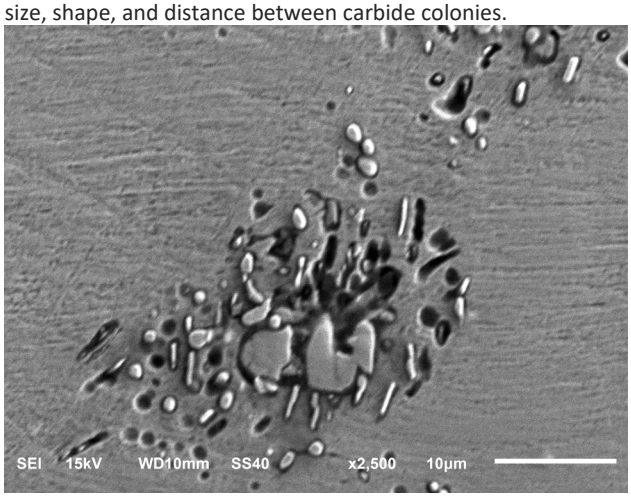

Figure 3 Morphology of dispersed hardened austenite formed through two-stage heating

The morphology of dispersed hardened austenite, which was generated via two-stage heating, is illustrated in Figure 3. The variation in the morphology of dispersed hardened austenite can be attributed to the non-uniform lamella thickness of the pearlite structure that is formed during the initial stage of heating. Consequently, the transformation of coarser pearlite lamellae into carbides exhibiting a completely round morphology is prolonged. The rate of carbide rounding in fine pearlite is greater than in coarse pearlite; the two types of pearlite are distinguished by their activation energies [15]. For enhancing the mechanical properties of austenitic manganese steel, a structure composed of finely dispersed, uniformly distributed cemented austenite carbide is optimal [16]. In the interim, during material preparation, grinding or refining may liberate carbide grains from this matrix. This indicates that the carbide granules are significantly harder than the matrix, allowing them to detach and create fissures in the matrix.

3.3 Macrostructure Observation of Heat Treatment Results

Observations of the macrostructure of materials that have undergone two-stage heating are carried out to determine the phenomena that occur in the material during plastic deformation by cold rolling. From the results of the macrophoto, it was recorded that the material began to experience crinkling on the surface that experienced cracks at the end of the cross section at a strain reduction (Ɛ) = 17.6% or at a thickness of 4.30 mm, as shown in Figure 4.

Figure 4 Macro photo of a sample that has been cold rolled on Ɛ = 17.6%

The crinkling on this part of the surface gets worse with increasing strain reduction, and cracks start to spread along the surface to the part of the cross section that contacts the rollers, as shown in Figure 5.

Figure 5 Macro photo of a sample that has been cold rolled on Ɛ = 53.6%. (a) the side that experiences a reduction in cross-section, (b) the part that contacts the roller

The phenomenon of crinkling in parts undergoing plastic deformation, followed by the formation of cracks, is called orange peeling [17]. According to him, the phenomenon of crinkling or orange peeling is grain boundary cracking, which is caused by the high concentration of carbon content in the part experiencing crinkling, so that this part tends to be more brittle, especially at the grain boundaries. Cracks can go into the specimen up to a certain depth, which depends on how the grains are arranged and how big they are, as well as on whether there are any barriers, like dispersed hardened austenite, in the way the cracks move.

In the current research, the orange peeling phenomenon is caused by the hardening of the surface. Rolling the material until it undergoes plastic deformation causes the first part of the surface to experience plastic deformation. It takes a very large amount of energy to directly deform a material to the inside. When rolling is repeated and the interior undergoes plastic deformation, it leads to excessive hardening on the surface. When you bend something plastically, it hardens because the austenite phase changes to the martensite phase. This is called the martensitic transformation.

3.4 Microstructure Observation of Heat Treatment Results

The microstructure of cold rolled samples is examined to see the shape of the austenite grains and the creation of the martensite phase owing to plastic deformation. As reported by Shih et al. (1955) in their study on the influence of the percentage of Mn on the martensite starting temperature, the high manganese and carbon elements in austenitic manganese steel prevent the formation of martensite during the heat treatment process by lowering the martensite starting temperature (Ms) to below 0°C [18].

Cold rolling, which causes the material to distort plastically, allows for the formation of the martensite structure in this study. Figure 6 shows an optical micrograph of austenitic manganese steel heat treated and rolled at a strain reduction of 54%. Martensite appears as a result of deformation. X-ray analysis also reveals structural changes in the austenitic manganese steel sample, which has been subjected to plastic deformation.

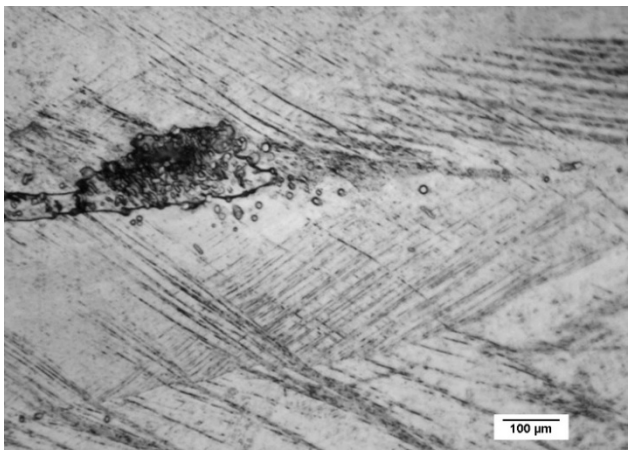

Figure 6 Microstructure of austenitic manganese steel with ε = 53.6%

Plastic deformation in austenitic manganese steel, leading to martensitic transformation, is caused by the cold work process that the FCC crystal structure in the steel undergoes. This process increases dislocations and stacking faults, which in turn affects the orientation of atoms in the lattice [19]. In addition to the formation of martensite caused by the cold rolling process, twin and slip can also develop in this particular type of cold-rolled austenitic manganese steel, as depicted in Figure 7. Stacking fault energy has a significant impact on the development of twin and slip in austenitic manganese steel. The stacking fault energy of austenitic manganese steel ranges from 20 to 40 mJ/m2 [20], enabling the production of twin and slides during plastic deformation. Furthermore, the size of the grains also has an impact on the creation of twin and slip. The twin mechanism is primarily responsible for deforming coarse austenite grains, while both the twin and slip processes contribute to the deformation of fine austenite grains [21].

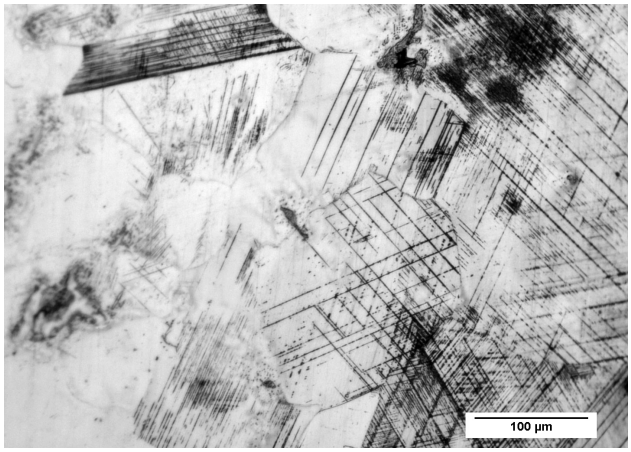

Figure 7 Microstructure of austenitic manganese steel with Ɛ = 5.2%

Previous research indicates that plastic deformation of austenitic manganese steel leads to a twin deformation strengthening mechanism [2], [17]. The formation of twin in austenitic manganese steel may occur within the martensite structure. Rolling induces a phase transformation in the martensite. The determination of twin in FCC is analogous to slip, as it is similarly governed by a specific slip system. In this case, the twin plane is located at (111) and the twin direction is <112> [11]. A twin is defined by the presence of a symmetrical reflection between two matrices. This dual system has a highly efficient impact on preventing slippage. The occurrence of the twin mechanism is also observed when the system experiences a small degree of slip and the critical resolved shear stress (CRSS) value increases. This leads to a lower twin formation mechanism compared to slip [11]. The deformation resulting from twinning exhibits a more straightforward mechanism in comparison to the process of martensite production. The absence of any alteration in the crystal structure occurs in the twin, with just a reconfiguration of the lattice's orientation taking place.

3.5 X-Ray Diffraction Test Analysis

X-ray diffraction (XRD) analysis was performed to provide evidence of the existence of martensite in the material that underwent cold rolling. Figure 8 displays the XRD test results of austenitic manganese steel sample that alone received heat treatment. The 2θ angle x-ray diffraction data correspond to the (111) γ, (200) γ, and (220) γ planes, which are part of the Face-Centered Cubic (FCC) plane. Additionally, the (220)α' plane belongs to the Body-Centered Cubic (BCC) plane of martensite. The presence of the alpha prime peak, which indicates the presence of martensite, is likely caused by friction during the sample cutting process and plastic deformation during grinding or polishing in the preparation stage of heat-treated samples.

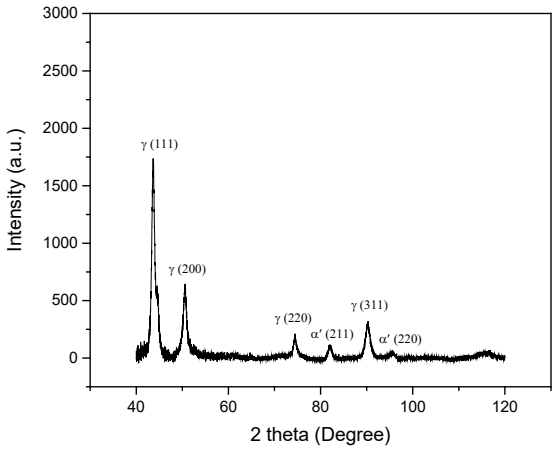

Figure 8 XRD test results on samples that have undergone heat treatment

Meanwhile, as illustrated in Figure 9, it can be noticed that the alpha-prime martensite angle increases in austenitic manganese steel that has undergone plastic deformation after the heat treatment process. Deformation in this type is similar to simple shear; in general, it is frequently characterized in terms of invariant plane strain since deformation includes volume changes normal to the invariant plane as well as shear. Invariant

plane strain is a homogenous distortion in which each point's displacement is in the same direction [19]. The magnitude of the displacement is proportional to the distance from the reference plane, which is a strain-free plane.

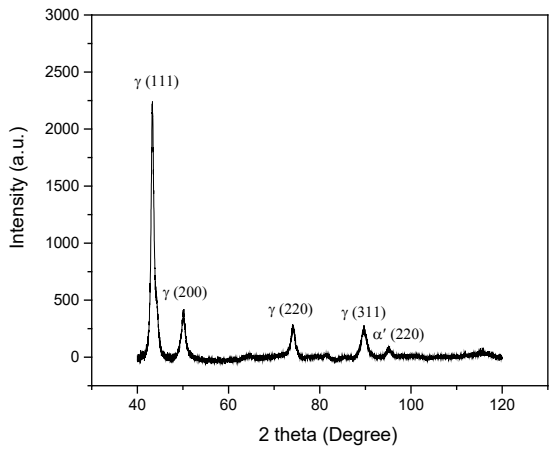

Figure 9 XRD test results on samples that have undergone heat treatment and cold rolling with a strain reduction of 54%.

3.6 Magnetic Test Analysis

The following properties are acquired from the video of qualitative magnetic testing by attaching a magnet to the specimen:

1. Non-magnetic cast material,
2. Non-magnetic heat-treated material,
3. As rolled material: magnetic.

Fe-Mn phase diagram for austenitic manganese steel with a manganese (Mn) content of 12.8 wt.% and the non-magnetic untransformed austenite phase [22]. Similarly, with heat-treated material, even though the decarburization process occurs, resulting in changes in the chemical composition on the surface of the specimen and producing magnetic properties on the surface, the material overall has non-magnetic properties because the magnetic properties are formed only on the surface. Only the surface is magnetic, and when the surface is cleansed, the magnetic qualities vanish. The magnetic characteristics of the as-rolled material are related to the martensite structure that occurs in the rolled specimen.

3.7 Hardness Test Analysis

The micro-Vickers hardness testing method was used with a load of 500 grams to perform hardness testing from the surface to the inside of the surface. Six of the 23 rolling samples were chosen, and one unrolled sample was chosen for hardness testing. The depth area from the surface is calculated for each sample in percentages ranging from 5% to 50% of the depth distance from the surface as shown in Table 1 and the graph in Figure 10 depicts the outcomes of hard testing.

Table 1 The depth of distance from the surface of hardness test sample

Condition	Test Method	Thickness (mm)	Distance from the surface (mm)				
			5 %	20 %	30 %	40 %	50 %
As-cast	Brinell	5.13	0.3	1.0	1.5	2.1	2.6
As-treated	Micro Vickers	5.13	0.3	1.0	1.5	2.1	2.6
As-rolled	Micro Vickers	4.71	0.2	0.9	1.4	1.9	2.4
As-rolled	Micro Vickers	4.38	0.2	0.9	1.3	1.8	2.2
As-rolled	Micro Vickers	4.16	0.2	0.8	1.2	1.7	2.1
As-rolled	Micro Vickers	3.62	0.2	0.7	1.1	1.4	1.8
As-rolled	Micro Vickers	3.37	0.2	0.7	1.0	1.3	1.7
As-rolled	Micro Vickers	3	0.2	0.6	0.9	1.2	1.5

The hardness test results on the as-cast samples had an average hardness value of 255 HB. With the help of the hardness conversion chart [23], the hardness value is equivalent to 262 HV. Either at 5% of the distance from the surface to the center of the sample or at 50% of the distance from the surface, the hardness value is relatively the same.

The hardness test results on materials that only received two-stage heating, or = 0%, indicate homogeneous hardness values. This is because mechanical treatment on austenitic manganese steel did not result in any strengthening, particularly on the austenite matrix. Hardness levels begin to rise in materials that have been mechanically treated with cold rolling. The hardness value in the cross section increases by 37% at = 8.5%, which is larger than the hardness of the material after only two stages of heating. The surface of the material is free of cracks in this condition. The hardness value increases with increasing strain reduction, reaching up to 132% harder than material heated in only two stages.

The strengthening of slip, twin, and martensitic transformation is responsible for the increase in hardness values in samples that have experienced plastic deformation employing the cold rolling method. This is also related to high surface hardness values because barriers exist in slip, twin, and martensite, and their quantity grows so that dislocations cannot migrate [11]. The high hardness value on this surface is related to rolling stress, which causes dislocations to travel to the outer surface and results in plastic deformation. These dislocations react with each other during movement, resulting in some that are easy to move and some that are difficult to move. Reaction products that are difficult to move will serve as a source of new dislocations, increasing dislocation density and making dislocation movement more difficult, hence increasing the material's strength.

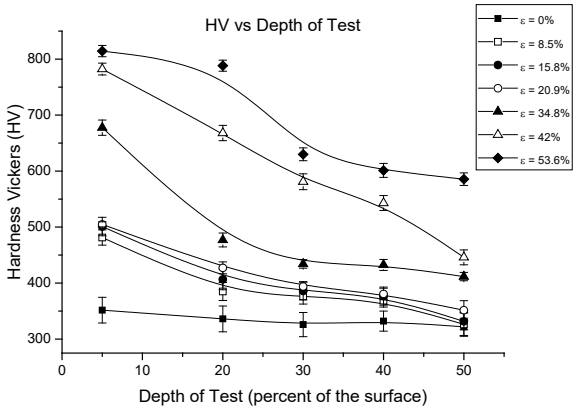

Figure 10 Graph of micro-Vickers hardness values for test samples that have been rolled and only heat treated

4.0 CONCLUSION

The plastic deformation process of austenitic manganese steel, which contains dispersed hardened austenite carbide, impacts the hardness value, which increases with decreasing strain. The production of martensite as a result of plastic deformation, as well as twinning, slip, and a reduction in grain shape, indicates that the material's hardness has increased. Before cracks appeared in the cross-section at = 8.5%, the material's hardness improved to 37% more than in the condition where only two phases of heating were performed. Even though cracks had spread across the cross-section, when rolling was continued to = 53.6%, the hardness increased 132% higher than in the condition where only two stages of heating were carried out.

Acknowledgement

We would like to express our gratitude to the Faculty of Engineering, Pasundan University, which has funded this research through the Internal Research Program and the Faculty of Mechanical and Aerospace Engineering, Bandung Institute of Technology, through the Thesis Fund Assistance Program.

Conflicts of Interest

The author(s) declare(s) that there is no conflict of interest regarding the publication of this paper

References

[1] D. K. Subramanyam, A. E. Swansiger, and H. S. Avery, 1990. *"Austenitic manganese steels*," ASM International.

[2] C. Chen, F. C. Zhang, F. Wang, H. Liu, and B. D. Yu, 2017. "Effect of N+ Cr alloying on the microstructures and tensile properties of Hadfield steel," *Materials Science and Engineering: A*, 679: 95–103.

[3] S. Hosseini and M. B. Limooei, 2011. "Optimization of heat treatment to obtain desired mechanical properties of high carbon Hadfield steels," *World Applied Science Journal*. 15(10): 1421–1424.

[4] Y. N. Dastur and W. C. Leslie, 1981. "Mechanism of work hardening in Hadfield manganese steel," *Metallurgical transactions A*, 12: 749–759,

[5] B. Hutchinson and N. Ridley, 2006. "On dislocation accumulation and work hardening in Hadfield steel," *Scripta Materialia*, 55(4): 299–302.

[6] Y. H. Wen, H. B. Peng, H. T. Si, R. L. Xiong, and D. Raabe, 2014. "A novel high manganese austenitic steel with higher work hardening capacity and much lower impact deformation than Hadfield manganese steel," *Material Design.* 55: 798–804.

[7] W. Yan, L. Fang, K. Sun, and Y. Xu, 2007. "Effect of surface work hardening on wear behavior of Hadfield steel," *Materials Science and Engineering: A*, 460: 542–549.

[8] W. Zhang, J. Wu, Y. Wen, J. Ye, and N. Li, 2010. "Characterization of different work hardening behavior in AISI 321 stainless steel and Hadfield steel," *Journal of Materal Science.* 45: 3433–3437.

[9] C. Chen, B. Lv, H. Ma, D. Sun, and F. Zhang, 2018. "Wear behavior and the corresponding work hardening characteristics of Hadfield steel," *Tribology International.* 121: 389–399.

[10] Ilham Lukman Nur Hakim and Budi Hartono Setiamarga, 2020. "*Study of The Effect Double Step Heat Treatment on the Mechanical Properties of Austenitic Manganese Steel ASTM A-128 Grade C,"* Bandung Institute of Technology, Bandung.

[11] G. E. Dieter and D. Bacon, 1976. *Mechanical metallurgy*.3. McGraw-hill New York.

[12] M. Sabzi, S. M. Far, and S. M. Dezfuli, 2018. "Effect of melting temperature on microstructural evolutions, behavior and corrosion morphology of Hadfield austenitic manganese steel in the casting process," *International Journal of Minerals, Metallurgy, and Materials*, 25: 1431–1438.

[13] S. Kuyucak, 2004. "Austenitic Manganese Steel Castings," in *Metallography and Microstructures*, 701–708. ASM International, doi: 10.31399/asm.hb.v09.a0003768.

[14] J. R. Davis, K. M. Mills, and S. R. Lampman, 1990. "Metals handbook. Vol. 1. Properties and selection: irons, steels, and high-performance alloys," *ASM International, 1063. Materials Park, Ohio 44073, USA.*

[15] A. Kamyabi-Gol and M. Sheikh-Amiri, 2010. "Spheroidizing kinetics and optimization of heat treatment parameters in CK60 steel using taguchi robust design," *Journal of Iron and Steel Research International*, 17(4): 45–52.

[16] H. Bhadeshia and R. Honeycombe, 2017. *Steels: microstructure and properties*. Butterworth-Heinemann.

[17] M. Abbasi, S. Kheirandish, Y. Kharrazi, and J. Hejazi, 2009. "The fracture and plastic deformation of aluminum alloyed Hadfield steels," *Materials Science and Engineering: A*, 513: 72–76.

[18] C. H. Shih, B. L. Averbach, and M. Cohen, 1955. "*Work Hardening and Martensite Formation in Austenitic Manganese Alloys*," Wright Air Development Center, Massachusetts Institute of Technology: Cambridge, MA, USA.

[19] H. Bhadeshia and C. M. Wayman, 2014. "Phase transformations: nondiffusive," in *Physical metallurgy*, 1021–1072. Elsevier.

[20] S. Allain, J.-P. Chateau, O. Bouaziz, S. Migot, and N. Guelton, 2004. "Correlations between the calculated stacking fault energy and the plasticity mechanisms in Fe–Mn–C alloys," *Materials Science and Engineering: A*, 387: 158–162.

[21] I. Karaman, H. Sehitoglu, A. J. Beaudoin, Y. I. Chumlyakov, H. J. Maier, and C. N. Tome, 2000. "Modeling the deformation behavior of Hadfield steel single and polycrystals due to twinning and slip," *Acta Mater*, 48(9): 2031–2047.

[22] G. Aggen *et al.*, 2005. "*ASM Handbook, Volume 1, Properties and Selection: Irons, Steels, and High Performance Alloys Section: Publication Information and Contributors Publication Information and Contributors Authors and Reviewers,"* ASM International.

[23] M. R. Sridhar and M. M. Yovanovich, 1996. "Empirical methods to predict Vickers microhardness," *Wear*. 193(1): 91–98.